

## Fusion of $^{32}\text{S} + ^{27}\text{Al}$ and $^{19}\text{F} + ^{40}\text{Ca}$ and the nucleus-nucleus potential

G. Doukellis

*Tandem Accelerator Laboratory, Nuclear Research Center Democritos, Aghia Paraskevi, Attikis, Greece*

(Received 7 January 1988)

The measured fusion-evaporation residue excitation functions for the systems  $^{32}\text{S} + ^{27}\text{Al}$  and  $^{19}\text{F} + ^{40}\text{Ca}$ , were parametrized in terms of a fusion barrier radius and a critical distance. The extracted radii, from this parametrization, agree with systematics. The extracted values for the nucleus-nucleus potential agree with the potentials that are based on the liquid drop model.

The measured fusion excitation functions, for lighter heavy ion systems, show three different regimes.<sup>1</sup> At low energies above the barrier, the fusion cross section  $\sigma_f$  follows the total reaction cross section. This region (I) is dominated by the interaction barrier. In region II the barrier penetrability is one and the two ions have to reach a smaller distance in order to fuse. This region has been described by the critical distance models.<sup>2-5</sup> At still higher energies  $\sigma_f$  shows a rather sudden drop with energy. This region (III) is characterized by a maximum angular momentum above which the incident waves do not fuse.

Several theoretical calculations<sup>2-11</sup> have been performed in order to fit the measured  $\sigma_f$  versus  $E^{-1}$ . The results of these calculations depend critically on the form of the nuclear potential which is used.

According to the simplest model,<sup>4,11</sup> the data in region I can be described by a straight line of the form

$$\sigma_f = \pi R_B^2 \left[ 1 - \frac{V(R_B, L=0)}{E_{\text{c.m.}}} \right], \quad (1)$$

where

$$V(r) = V_C(r) + V_N(r) \quad (2)$$

is the interaction potential, which is the sum of the Coulomb and nuclear potentials.  $R_B$  and  $V(R_B)$  are the fusion radius and fusion barrier height, respectively. By fitting a large class of data,  $R_B$  was found to be

$$R_B = r_B (A_1^{1/3} + A_2^{1/3}) \quad \text{with } r_B = 1.4 \text{ fm} . \quad (3)$$

$A_1$  and  $A_2$  are the mass numbers of the target and the projectile.

In region II, according to the critical distance models,<sup>4</sup> a similar relationship between  $\sigma_f$  and  $E^{-1}$  exists:

$$\sigma_f = \pi R_C^2 \left[ 1 - \frac{V(R_C, L=0)}{E_{\text{c.m.}}} \right]. \quad (4)$$

$R_C$  is the critical distance expressed in terms of a universal critical parameter  $r_C$ , suggested by Galin *et al.*:<sup>2</sup>

$$\begin{aligned} R_C &= r_C (A_1^{1/3} + A_1^{1/3}), \\ r_C &= 1.0 \pm 0.07 \text{ fm} . \end{aligned} \quad (5)$$

$V(R_C)$  is the value of the interaction potential at  $R_C$ . Whereas the description of region I in terms of Eq. (1) has not been disputed, the validity of Eq. (4) and the physical origin of a critical distance have been questioned.<sup>8,10</sup>

Region III can be described by a line of the form

$$\sigma_f = \frac{\pi \hbar^2}{2\mu} L_m^2 E^{-1} . \quad (6)$$

Here the fusion-evaporation cross section is limited either by the maximum angular momentum  $L_m$ , in the entrance channel that leads to fusion, or by the maximum angular momentum  $L_m$ , beyond which the compound nucleus fissions.

Figure 1 shows the measured fusion-evaporation excitation function for the system  $^{32}\text{S} + ^{27}\text{Al}$ . The data for  $E_{\text{lab}} = 67-132.5$  MeV were taken from Ref. 11, for  $E_{\text{lab}} = 142-227$  MeV from Refs. 12 and 13, and for  $E_{\text{lab}} = 320-393$  MeV from Refs. 14 and 15. Figure 2 shows the  $^{19}\text{F} + ^{40}\text{Ca}$  fusion-evaporation residue excitation function measured in Ref. 14. Both fusion reactions lead to the same compound nucleus  $^{59}\text{Cu}$ . We see that both systems exhibit the three regions that were mentioned above. Each region looks well defined, and in ad-

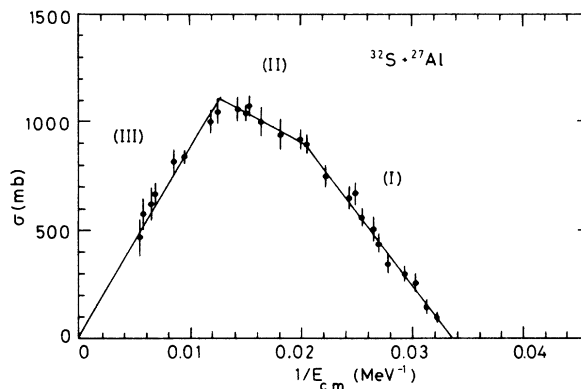


FIG. 1. The measured fusion-evaporation residue excitation function for the system  $^{32}\text{S} + ^{27}\text{Al}$ . The lines are the result of least-squares fits through the data points. The symbols (I), (II), and (III) denote the regions (I), (II), and (III) discussed in the text.

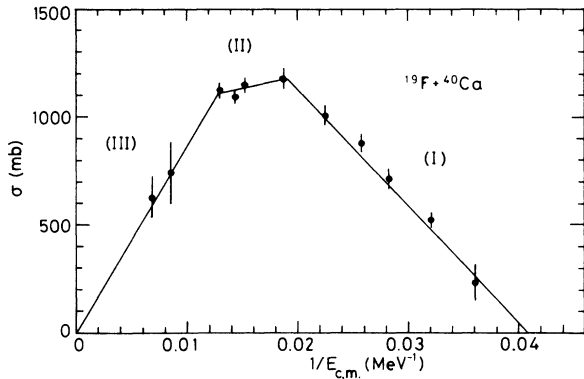


FIG. 2. Same as in Fig. 1, but for the system  $^{19}\text{F} + ^{40}\text{Ca}$ .

dition the data within each region follow a straight line. Thus the observed variation of  $\sigma_f$  vs  $E^{-1}$ , for the systems  $^{32}\text{S} + ^{27}\text{Al}$  and  $^{19}\text{F} + ^{40}\text{Ca}$ , seems to obey the linear relationships expressed by Eqs. (1), (4), and (6).

The lines shown in Figs. 1 and 2 are the result of least-squares fits through the data points. The parameters extracted from those fits, for regions I and II, give  $R_B$ ,  $V(R_B)$ ,  $R_C$ , and  $V(R_C)$  according to Eqs. (1) and (4).

Table I lists them in columns 3 and 6 together with the corresponding correlation coefficient  $r$ , which is listed in the last column. We see that the correlation coefficient is particularly high for all lines except the one for the  $^{19}\text{F} + ^{40}\text{Ca}$  system in region II, where it is relatively low because of poor statistics. Columns 4 and 5 of Table I list the radius parameters extracted from the data and from systematics, respectively. We see that the fusion radius parameters agree with the value 1.4 fm of Eq. (3), and the critical radius parameters agree with the value  $1.0 \pm 0.07$  fm of Eq. (5).

From Eq. (2) we see that the nuclear part of the potential can be obtained by subtracting from the extracted value of the interaction potential (column 6 of Table I), the value of the Coulomb potential. For the Coulomb potential we used the potential suggested in Ref. 16. The values for the nuclear potential, derived in this manner, are listed in column 7 of Table I.

Figures 2 and 3 show the nuclear potential as a function of the distance, calculated by several potential models, together with the values for the nuclear potential and separation distance of Table I. We observe a good agreement between the values of the nuclear potential extracted from the measured excitation functions and the modified proximity potential,<sup>17,6</sup> the Wilczynski poten-

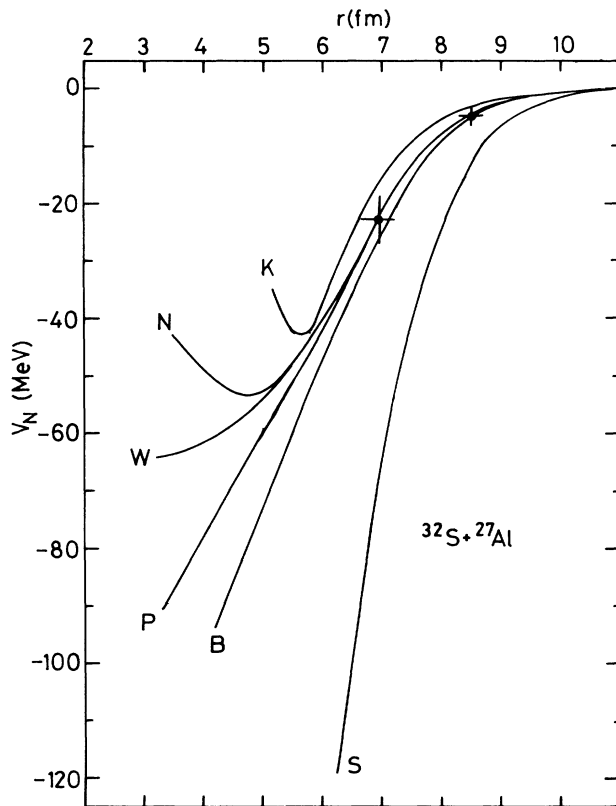


FIG. 3. The nuclear potential as a function of the distance for the system  $^{32}\text{S} + ^{27}\text{Al}$ . The letters  $K$ ,  $N$ ,  $W$ ,  $P$ ,  $B$ , and  $S$ , stand for the Krappe-Nix-Sierk potential, the Ngo potential, the Wilczynski potential, the modified proximity potential, the Bass potential, and the single-folding potential, respectively. The data points are from Table I.

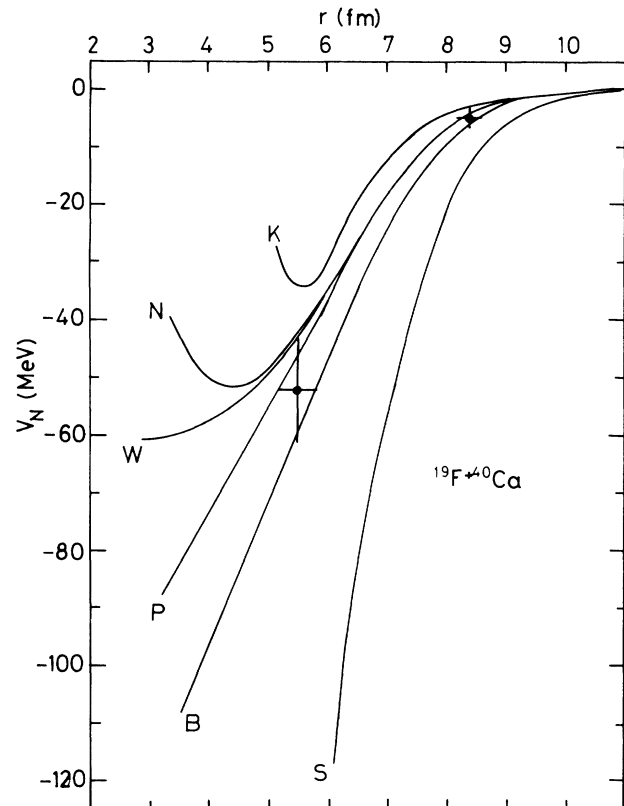


FIG. 4. Same as in Fig. 3, but for the system  $^{19}\text{F} + ^{40}\text{Ca}$ .

TABLE I. Fusion parameters extracted from the least-squares fits discussed in the text.

Heavy ion system	Region	$R$ (fm)	$r_0$ (fm)	$r_0^a$ (fm)	$V(R)$ (MeV)	$V_N(R)$ (MeV)	$r$
$^{32}\text{S} + ^{27}\text{Al}$	I	$8.5 \pm 0.2$	$1.38 \pm 0.03$	1.4	$29.7 \pm 2.0$	$-4.4 \pm 2.0$	-0.99
	II	$6.9 \pm 0.3$	$1.11 \pm 0.05$	$1.0 \pm 0.07$	$19.3 \pm 4.0$	$-23.0 \pm 4.0$	-0.97
$^{19}\text{F} + ^{40}\text{Ca}$	I	$8.4 \pm 0.2$	$1.38 \pm 0.03$	1.4	$24.3 \pm 2.0$	$-5.0 \pm 2.0$	-0.99
	II	$5.5 \pm 0.3$	$0.91 \pm 0.05$	$1.0 \pm 0.07$	$-14.0 \pm 9.0$	$-52.0 \pm 9.0$	0.82

<sup>a</sup>From systematics.

tial,<sup>18</sup> the Ngo potential,<sup>19</sup> and the Bass potential.<sup>20</sup> The agreement with the Krappe-Nix-Sierk potential<sup>21</sup> is not good for  $r=5.5$  fm. It should be noted that, for all of the above potential models, the potential strength was calculated on the basis of some form of a liquid drop model, but the potential shape was obtained using a different method in each one of them. In Figs. 3 and 4 we present also the single-folding potential of Gross and Kalinowski.<sup>22</sup> The data points do not agree with the single-folding potential even at distances close to the fusion barrier ( $r \sim 8.5$  fm) where the validity of Eq. (1) is well established.

In region III the slope of the straight line corresponds to  $L_{\text{max}} = 44\hbar$  for both systems. From the rotating liquid drop model<sup>23</sup> we get the angular momentum at which the fission barrier becomes equal to the proton barrier in the compound nucleus  $^{59}\text{Cu}$ ,  $L = 45\hbar$ . This means that in re-

gion III the fusion-evaporation cross section is limited by the fission stability of the compound nucleus. A more detailed discussion about region III may be found in Ref. 13.

In conclusion, the observed  $^{32}\text{S} + ^{27}\text{Al}$  and  $^{19}\text{F} + ^{40}\text{Ca}$  excitation functions can be described in a simple way by three straight lines. The lines in regions I and II are determined by the form of the nucleus-nucleus potential at the fusion barrier radius and the critical distance radius, respectively. The radii extracted from the data agree with systematics and the values extracted for the nucleus-nucleus potential agree with the potentials whose strength was calculated from the liquid drop model. The results of the present analysis support the validity of the critical distance model and demonstrate the use of fusion reactions as a tool in probing the nucleus-nucleus potential at small distances.

- <sup>1</sup>U. Mosel, in *Heavy Ion Collisions*, edited by Bock (North-Holland, New York, 1980), p. 338.
- <sup>2</sup>J. Galin, D. Guerreau, M. Lefort, and X. Tarrago, *Phys. Rev. C* **9**, 1018 (1974).
- <sup>3</sup>J. B. Natowitz, E. T. Chulik, and M. N. Namboodiri, *Phys. Rev. C* **6**, 2133 (1972).
- <sup>4</sup>D. Glas and U. Mosel, *Nucl. Phys. A* **237**, 429 (1975); *Phys. Rev. C* **10**, 2620 (1974).
- <sup>5</sup>R. Bass, *Nucl. Phys. A* **231**, 45 (1974).
- <sup>6</sup>J. R. Birkelund, L. E. Tubbs, J. R. Huizenga, J. N. De, and D. Sperber, *Phys. Rep.* **56**, 107 (1979).
- <sup>7</sup>S. Biornholm and W. J. Swiatecki, *Nucl. Phys. A* **391**, 471 (1982).
- <sup>8</sup>M. Blann and D. Akers, *Phys. Rev. C* **26**, 465 (1982).
- <sup>9</sup>P. Frobrich, *Phys. Rep.* **34**, 552 (1984).
- <sup>10</sup>S. M. Lee, T. Matsuse, and A. Arima, *Phys. Rev. Lett.* **45**, 165 (1980).
- <sup>11</sup>H. H. Cutbrod, W. G. Winn, and M. Blann, *Nucl. Phys. A* **213**, 267 (1973).
- <sup>12</sup>F. Porto, S. Sambataro, K. Kusterer, Liu Ken Pao, G. Doukellis, and H. L. Harney, *Nucl. Phys. A* **375**, 237 (1981).
- <sup>13</sup>G. Doukellis, G. Hlawatsch, B. Kolb, A. Miczaika, G. Ros-

ner, and B. Sedelmeyer (unpublished).

- <sup>14</sup>G. Rosner, J. Pochodzalla, B. Heck, G. Hlawatsch, A. Miczaika, H. J. Rabe, R. Butsch, B. Kolb, and B. Sedelmeyer, *Phys. Lett.* **150B**, 87 (1985).
- <sup>15</sup>R. L. Kozub, N. H. Lu, J. M. Miller, D. Logan, T. W. Debiak, and L. Kowalski, *Phys. Rev. C* **11**, 1497 (1975).
- <sup>16</sup>J. R. Bondorf, M. I. Sobel, and D. Sperber, *Phys. Rep. C* **15**, 83 (1974).
- <sup>17</sup>J. Randrup, *Nucl. Phys. A* **307**, 319 (1978).
- <sup>18</sup>B. Wilczynski and K. Siwel-Wilczynska, *Phys. Lett.* **55B**, 270 (1975).
- <sup>19</sup>C. Ngo, in *Proceedings of the International Conference in Nuclear Physics, Florence, 1983*, edited by P. Blasi and R. A. Ricci (Tipografia Compositori, Bologna, 1983), Vol. II, p. 321.
- <sup>20</sup>R. Bass, *Phys. Rev. Lett.* **39**, 265 (1977).
- <sup>21</sup>H. J. Krappe, J. R. Nix, and A. J. Sierk, *Phys. Rev. Lett.* **42**, 215 (1979).
- <sup>22</sup>D. H. E. Gross and H. Kalinowski, *Phys. Rep. C* **45**, 175 (1978).
- <sup>23</sup>S. Cohen, F. Plasil, and W. J. Swiatecki, *Ann. Phys. (N.Y.)* **82**, 557 (1974).